Perturbation of Retinoid Homeostasis Increases Malformation Risk in Embryos Exposed to Pregestational Diabetes

Short title: Retinoid Homeostasis in Diabetic Embryopathy

Leo M.Y. Lee,[1,2,3] Maran B.W. Leung[1], Rachel C.Y. Kwok[1], Yun Chung Leung[3], Chi Chiu Wang[1,2,4], Peter J. McCaffery[5], Andrew J. Copp[6] and Alisa S.W. Shum[1]

[1]School of Biomedical Sciences, Faculty of Medicine, The Chinese University of Hong Kong

[2]Department of Obstetrics and Gynaecology, Faculty of Medicine, The Chinese University of Hong Kong, Hong Kong

[3]Department of Applied Biology and Chemical Technology, The Hong Kong Polytechnic University, Hong Kong

[4]Li Ka Shing Institute of Health Sciences, Faculty of Medicine, The Chinese University of Hong Kong, Hong Kong

[5]Institute of Medical Sciences, University of Aberdeen, Aberdeen, UK

[6]Newlife Birth Defects Research Centre, Institute of Child Health, University College London, London, UK

Corresponding author:

Alisa S.W. Shum, alisa-shum@cuhk.edu.hk

ABSTRACT

Pregestational diabetes is highly associated with an increased risk of birth defects. However, factors that can increase or reduce the expressivity and penetrance of malformations in pregnancies in women with diabetes remain poorly identified. All-*trans* retinoic acid (RA) plays crucial roles in embryogenesis. Here, we find that *Cyp26a1*, which encodes a key enzyme for catabolic inactivation of RA required for tight control of local RA concentrations, is significantly downregulated in embryos of diabetic mice. Embryonic tissues expressing *Cyp26a1* show reduced efficiency of RA clearance. Embryos exposed to diabetes are thus sensitized to RA and more vulnerable to the deleterious effects of increased RA signalling. Susceptibility to RA teratogenesis is further potentiated in embryos with a preexisting genetic defect of RA metabolism. Increasing RA clearance efficiency using a preconditioning approach can counteract the increased susceptibility to RA teratogenesis in embryos of diabetic mice. Our findings provide new insight into gene-environment interactions that influence individual risk in the manifestation of diabetes-related birth defects and shed light on the environmental risk factors and genetic variants for a stratified medicine approach to screening women with diabetes who are of childbearing age and assessing the risk of birth defects during pregnancy.

Offspring of women with pregestational diabetes show a markedly increased risk of birth defects (1). While the cause of diabetic embryopathy is known to be multifactorial, previous investigations focused mainly on the effect of maternal diabetes alone on the embryo. Genetic and environmental factors that can influence the expressivity and penetrance of congenital malformations in pregnancies in women with diabetes remain far from clear (2,3). Interestingly, some malformations found in the offspring of mothers with diabetes (4-6) are very similar to those anomalies arising from exposure to excess retinoids (vitamin A and its analogues) in humans and animals (7-9). For instance, a large-scale study of 18 population-based congenital anomaly registries shows that the odds ratio for caudal regression in pregnancies in women with versus without diabetes (odds ratio 26.4; 95% CI 8.98-77.64) is well above that of other malformations (4), which strengthens the conclusion of previous studies that caudal regression is a characteristic anomaly associated with pregnancy in women with diabetes (5,6). Caudal regression also commonly occurs with retinoid teratogenesis in animal studies (9-11).

Many of the functions of vitamin A in embryogenesis are mediated via its metabolite all-*trans* retinoic acid (RA), which is a key signaling molecule controlling the development of multiple organ systems. Different embryonic tissues/organs show variations in requirements for RA; thus tight regulation of local RA concentrations is critical to ensure the precise levels of RA signaling required for normal embryo development. An important mechanism to control local RA concentrations is via catabolic inactivation by the CYP26 enzymes belonging to the cytochrome P450 family. Three *Cyp26* genes-namely *Cyp26a1*, *Cyp26b1*, and *Cyp26c1*-are expressed in specific embryonic tissues and attenuate the deleterious effects of excessive RA signalling.

Among them, CYP26A1 is the key RA catabolizing enzyme in many tissues and the only subtype that is expressed in the tailbud region of the embryo (12), where caudal regression arises (11). Homozygous deletion of *Cyp26a1* in mice is lethal in mid- to late gestation, with embryos exhibiting caudal truncation (13,14). Similarly, we and others have demonstrated that mouse embryos exposed to excess RA develop caudal truncation and various phenotypes, including specific renal, anorectal, caudal spinal cord, and lower extremity malformations (10,11,15) commonly associated with caudal regression in humans (16,17). Moreover, we found that maternal diabetes potentiates the effect of RA to cause caudal regression in mice (18). This similarity in phenotypes resulting from genetic and environmental disturbances therefore led us to speculate that maternal diabetes may perturb embryonic CYP26A1 function in maintaining the tight regulation of local RA concentrations in specific tissues. We hypothesized that such tissues would be vulnerable to a perturbation of RA levels and exhibit increased susceptibility to RA teratogenesis. Here, we provide evidence to support this hypothesis using a mouse model of pregestational diabetes. Notably, our findings show that interaction between a genetic predisposition and an environmental agent to disrupt RA homeostasis can potentiate maternal diabetes-induced deregulated RA catabolism in increasing the risk for malformation.

RESEARCH DESIGN AND METHODS

Animals

All animal experimentation was conducted following the guidelines set by The Chinese University of Hong Kong. Diabetes was induced in female ICR mice by streptozotocin injections according to established protocols (18). Mice with a blood glucose concentration ≥16.7 mmol/L were classified as manifestly diabetic (MD). Untreated, age-matched female ICR mice were used as the nondiabetic (ND) control. Mice were kept in a 12-h light/12-h dark cycle; the light cycle commenced at 11:00 $_{A.M.}$ Pregnancies were obtained by timed mating for 2 h (9:00-11:00 $_{A.M.}$) between MD/ND female ICR mice and male ICR mice, or male *Cyp26a1*$^{+/-}$ mice in a 129/C57BL/6Cr/DBA mixed background (a gift from Prof. Hamada [14]). The time of finding a copulation plug at 11:00 $_{A.M.}$ was defined as embryonic day (E) 0. Mice were checked for blood glucose levels before embryo collection to confirm that MD mice remained diabetic during pregnancy (Supplementary Table 1).

Gene Expression

Whole embryos were subjected to in situ hybridization for *Cyp26a1*, *Cyp26b1*, or *Cyp26c1* with digoxygenin-labeled RNA probes (19). The mRNA expression levels of various genes were determined using real-time quantitative RT-PCR. To minimize differences in expression levels resulting from variations in the developmental stage, only embryos within the same somite range (somite stage 9-10 for E8 embryos; somite stage 19-21 for E9 embryos) in each litter were collected. This criterion was adopted for

embryo collection in other experiments. For crossing between male and female ICR mice, all embryos at the appropriate somite stage from the same litter were pooled as one sample. For crossing between male *Cyp26a1*$^{+/-}$ and female ICR mice, individual embryos were collected. After DNA genotyping of the yolk sac using PCR with primers as previously described (14), embryos of the same genotype (*Cyp26a1*$^{+/+}$ or *Cyp26a1*$^{+/-}$) from the same litter were pooled as one sample. Total RNA was extracted from the whole embryo or tailbud (defined as the caudal end of the embryo up to one somite length posterior to the last somite) samples using the FavorPrep Tissue Total RNA Mini Kit (Favorgen Biotech Corp.). An equal amount of RNA (250 ng) was reverse-transcribed into first-strand cDNA using a High-Capacity cDNA Reverse Transcription Kit (Applied Biosystems). The cDNA yielded from reverse transcription of 1.67 ng RNA was subjected to quantitative PCR using ABI 7900HT Fast Real-Time PCR system (Applied Biosystems), with SYBR Green PCR Master Mix (Applied Biosystems). *β-actin* was used as the internal control for normalization. The PCR conditions and primer sequences were listed in Supplementary Table 2.

In Vitro RA Degrading Efficiency

Using an assay modified from Yamamoto et al. (20), four tailbuds of E9 embryos from the same litter were pooled as one sample and lysed in 5 μL of DMEM by trituration with a pipette tip, followed by five cycles of freezing in liquid nitrogen and thawing in a water bath at 37^{o}C for 1 min. The whole lysate was added to 50 μL of a reaction mixture containing 50 nmol/L all-*trans* RA (Sigma-Aldrich), with or without 1.6 mg/mL NADPH (a cofactor of the cytochrome P450 enzyme), 0.3 mg/mL dithiothreitol (DTT; a reducing agent for optimal cytochrome P450 enzyme function), and the CYP26-specific inhibitor

R115866 (21) at a concentration of 1, 10, or 100 nmol/L in a culture medium (DMEM supplemented with 10% FBS). The reaction mixture was then incubated in a 5% CO_2 incubator at 37^{o}C for 2 h, during which the exogenous RA in the medium was degraded by the RA-catabolizing enzyme in the tailbud lysate. After incubation, the amount of RA remaining was determined by adding the reaction mixture, diluted 30-fold with the culture medium, in triplicate to a 96-well plate containing RA reporter cells, which are F9 cells transfected with an RA response element that drives β-galactosidase expression (22). Serially diluted RA standard solutions at concentrations from 10^{-6} to 10^{-11} mol/L were added in triplicate to the same 96-well plate. After culturing for 24 h, cells were stained with X-gal and the intensity of the blue product was measured using a microplate spectrophotometer. RA in the sample was quantified using a standard curve constructed with the serially diluted RA solutions (Supplementary Fig. 1).

In Vivo Clearance of RA

To determine the in vivo efficiency of RA clearance, the tailbud was collected under dim yellow light at various time points after injection of RA (50 mg/kg body weight) at E9, Tailbuds were individually placed in 300 μL of the culture medium, with 100 nmol/L R115866 added to inhibit endogenous CYP26 enzymes. After 24 h of incubation in 5% CO_2 at 37^{o}C to allow maximum release of RA from the tailbud into the medium, RA in the medium was quantified using the RA reporter cell line. A preliminary study demonstrated that the culture conditions did not cause significant degradation of RA (Supplementary Fig. 2). To validate that RA measurements using the RA reporter cell line indeed measure RA released from tissues that can modulate RA levels, the tailbuds

of E9 embryos were collected 3 h after injection of RA. The midbrain, which does not express any *Cyp26* genes in untreated or RA-treated conditions, was also collected from these embryos as a control. Tissues from the same litter were pooled as one sample. RA in the sample was quantified using high-performance liquid chromatography (23).

Detection of Bioactive RA in Tailbuds

The caudal-most portion of the tailbuds of E9 embryos of MD and ND mice was excised under dim yellow light and individually placed on top of RA reporter cells grown on a 96-well plate in the culture medium, with 100 nmol/L R115866 added to inhibit endogenous CYP26 enzymes. After 24 h of culture, cells were stained with X-gal. The number of positively stained cells around the tailbud explant was counted under a stereomicroscope.

Susceptibility to RA Teratogenesis

The teratogenic effect of RA is dose- and stage-dependent (9). To determine susceptibility to RA teratogenesis, MD or ND mice at E8 or E9 received an intraperitoneal injection of 25 mg/kg RA or an equivalent volume of suspension vehicle (peanut oil) as a control, and their embryos were examined at E13. Embryos treated with RA at E9 were examined for the extent of caudal truncation, which was expressed as the ratio of tail length (TL) to crown-rump length (CRL), as used in our previous studies (18). Embryos treated with RA at E8 were examined for exencephaly and spina bifida. Near-term E18 fetuses from MD or ND mice injected with 40 mg/kg RA at E9 were examined for various renal malformations, as described in our previous studies (24).

Maternal preconditioning with low-dose RA (0.625 or 1.25 mg/kg) or suspension vehicle (peanut oil) as a control was achieved by oral gavage 2 h before administering an intraperitoneal injection of a teratogenic dose of RA.

Statistics

Statistical differences between two groups were analyzed by the unpaired Student *t* test. Differences between multiple groups of data were analysed using one-way ANOVA, followed by the Bonferroni post hoc test, or using the contrast test to assess the extent of differences. Dose response was analyzed using linear regression. The best-fit curves were compared using nonlinear regression. Data were presented as mean ± SEM, with $P < 0.05$ considered as statistically significant. All statistical analyses were conducted using SPSS software (SPSS Inc.), except nonlinear regression analysis, which was conducted using Prism software (GraphPad Software).

RESULTS

Cyp26a1 Expression Levels and RA Degrading Efficiency Are Reduced in Embryos of Diabetic Mice

During early mouse postimplantation development, *Cyp26a1* is initially expressed in the headfold mesenchyme (Fig. 1*A*), and then extends to the caudal neural plate and primitive streak (Fig. 1*B*). As development proceeds, *Cyp26a1* expression persists at the caudal end (Fig. 1*C* and *D*), now called the tailbud, which contains progenitor cells for forming various posterior structures. Rostrally, it is expressed in the craniofacial, cervical, and branchial arch mesenchyme (Fig. 1*C*). Embryos of MD mice exhibit a significant decrease in *Cyp26a1* mRNA transcripts in all of these regions compared with embryos of ND mice (Fig. 1*A*-*E*). In contrast, *Cyp26b1* and *Cyp26c1* are expressed predominantly in the cranial region but not in the tailbud (Fig. 1*F* and *H*), and show no significant difference in expression levels between embryos of MD and ND mice (Fig. 1*G* and *I*).

To determine whether a decrease in *Cyp26a1* expression results in reduced efficiency of RA catabolism, we used an in vitro assay to compare the RA-degrading efficiency of the tailbud, which exclusively expresses *Cyp26a1*, but not *Cyp26b1* and *Cyp26c1*, from E9 embryos of MD and ND mice. Results showed that only a low level of RA-degrading activity was detected when tailbud lysate alone was applied (Fig. 2*A*). However, in the presence of NADPH and DTT for optimal activity of CYP26 enzymes, 66% of added RA was degraded within 2 h. In contrast, cotreatment with 1-100 nmol/L of R115866, a potent CYP26-specific inhibitor (21), resulted in significant

dose-dependent inhibition of RA degradation. Notably, while there was no significant difference in the protein content of the tailbuds excised from embryos of MD and ND mice (Supplementary Fig. 3), tailbud lysate of the MD group exhibited only 45% of the activity of the ND group.

To further compare the efficiency of in vivo clearance of RA, MD and ND mice were injected with an exogenous dose of RA (50 mg/kg) at E9; then RA in individual tailbuds was measured at hourly intervals using the RA reporter cell line (Fig. 2*B*), which showed results comparable with those from quantification of RA using high-performance liquid chromatography (Supplementary Table 3). Despite a similar response time course in the MD and ND groups, the amount of RA in tailbuds of the MD group was significantly higher than in the ND group at all time points studied (Fig. 2*B*). Moreover, by determining the area under the concentration-time curve (AUC), which is considered as the most appropriate pharmacokinetic correlate of embryotoxicity of RA (25), there was a twofold difference between the MD ($AUC_{0\text{-}8h}$: 25.59 nmol/L X h, calculated using Prism 5 software [GraphPad Software]) and the ND ($AUC_{0\text{-}8h}$: 12.70 nmol/L X h) groups, implying that the efficiency of in vivo RA clearance in tailbuds of embryos exposed to diabetes was reduced by 50%. By contrast, the E9 midbrain, which does not express any of the three *Cyp26* genes in both untreated and RA-treated conditions (Supplementary Fig. 4*A*), exhibited no difference in RA levels between embryos of MD and ND mice at 3 h after the injection of RA (Supplementary Fig. 4*B*).

RA Levels Are Increased in Tailbuds of Embryos of Diabetic Mice

To determine whether reduction in RA-degrading efficiency would lead to an increase in

endogenous RA levels, we excised the caudal-most portion of the tailbud (Fig. 3*A*) farthest from the RA source in adjacent trunk tissues, and put it directly on the RA reporter cells to detect bioactive RA release (22). Reporter cells exposed to RA expressed β-galactosidase and turned blue with X-gal staining. There were hardly any positively stained cells around tailbuds from embryos of ND mice (Fig. 3*B* and *C*), which agrees with previous findings that the tailbud is normally devoid of RA (26). However, stained cells were observed around more than half the tailbuds from embryos of MD mice. The number of stained cells varied from fewer than 10 to more than 40, implying a varying magnitude of elevation of RA level in tailbuds of embryos exposed to diabetes.

Several genes including *Fgf8*, *Wnt3a*, and *Cdx2*, are indispensable key players in caudal development (27). Excessive RA has been demonstrated to downregulate these genes and cause axial truncation (11,26,28). Of these genes, however, only *Fgf8* was significantly downregulated in the tailbuds of embryos of MD mice (Fig. 4*A*). It is possible that the magnitude of increase in RA levels may not have reached the threshold for causing a detectable alteration in the expression of some of these genes. We therefore challenged embryos with 50 mg/kg of RA to test whether deregulated catabolism of RA would sensitize embryos of MD mice to RA. A dramatic increase in mRNA levels of *Cyp26a1* in the tailbud occurred 4 h after injection of RA (Fig. 4*B*), showing that *Cyp26a1* is highly inducible by RA. However, the magnitude of upregulation of *Cyp26a1* in tailbuds of the MD group was significantly less than that in the ND group ($P < 0.05$, contrast test), which further exacerbated the difference between these two groups. Concomitantly, there was a marked downregulation of *Fgf8*, with expression levels in tailbuds of the RA-treated MD group reduced to less than one-third of that in the ND group without RA treatment (Fig. 4*C*). Consistent with our previous findings (18), though

there was no difference in *Wnt3a* expression levels between the tailbuds of MD and ND groups at a steady state (Fig. 4*A*), upon RA challenge *Wnt3a* was downregulated to a significantly greater extent in tailbuds of the MD group than those of the ND group (Fig. 4*C*). Similarly, the MD group showed an increased propensity toward RA-induced downregulation of *Cdx2*.

RA action is mediated via transactivation by retinoic acid receptors (RARs) that heterodimerize with retinoid X receptors (RXRs). In the mouse embryo, Rarγ and Rxrα mediate the teratogenic effect of RA in inducing caudal truncation (29,30). However, there were no differences in expression levels of *Rarγ* and *Rxrα* between the tailbuds of embryos of ND and MD mice at a steady state (Fig. 4*A*) or 4 h after injection of RA (Fig. 4*C*). Together, these findings support the idea that enhanced downregulation of caudal regulatory genes in the tailbuds of embryos of MD mice is due to increased RA levels resulting from the reduced efficiency of RA degradation, rather than secondary to differences in the efficiency of transactivation via RA nuclear receptors.

Genetic Reduction of *Cyp26a1* Exacerbates the Susceptibility of Embryos of Diabetic Mice to RA Teratogenesis

We asked whether a decrease in *Cyp26a1* expression leads directly to reduced efficiency of RA clearance, and whether functional loss of *Cyp26a1* could interact with the maternal diabetic environment to influence RA-degrading efficiency and susceptibility to RA teratogenesis. To investigate these questions, we crossed *Cyp26a1*$^{+/-}$ male mice with MD or ND female mice. We hypothesized that *Cyp26a1*$^{+/-}$ mutant embryos would exhibit a lower RA-degrading efficiency than their *Cyp26a1*$^{+/+}$ wild-type littermates and that exposure to maternal diabetes would exacerbate these genetic differences.

Indeed, E9 embryos from different genotype-maternal environment combinations showed prominent differences in *Cyp26a1* levels (Fig. 5*A*). The *Cyp26a1* mRNA levels in tailbuds of *Cyp26a1*$^{+/-}$ embryos of MD mice were reduced to half of the level in *Cyp26a1*$^{+/+}$ embryos of ND mice (Fig. 5*B*), with a corresponding decrease in CYP26-mediated RA-degrading efficiency (Fig. 5*C*). When RA levels were increased via maternal challenge with 25 mg/kg of RA, a 50% reduction in *Cyp26a1* expression levels and RA-degrading efficiency in tailbuds of *Cyp26a1*$^{+/-}$ embryos of MD mice resulted in exposure to an eightfold higher effective concentration of RA in comparison with tailbuds of *Cyp26a1*$^{+/+}$ embryos of ND mice (Fig. 5*D*). This effect was noted 3 h after RA injection, when accumulation of RA had reached its peak (Fig. 2*B*). In agreement with these findings, *Cyp26a1*$^{+/-}$ embryos of MD mice were most sensitized to RA-induced caudal truncation (Supplementary Fig. 5), as indicated by the smallest ratio of TL to CRL (Fig. 5*E*). The TL-to-CRL ratio was used as a "surrogate" both for the regression of multiple caudal structures in mice and for the analogous "caudal regression" process that affects species without tails, such as humans. In addition to caudal truncation, renal malformations are commonly associated with caudal regression (15,16). Indeed, we also found a 12-fold increase in the incidence (Fig. 5*F*) and severity (Table 1) of renal malformations in near-term *Cyp26a1*$^{+/-}$ fetuses exposed to maternal diabetes compared with wild-type fetuses in pregnancies in nondiabetic mice when challenged with a teratogenic dose of RA.

Enhancing RA-Degrading Efficiency Counteracts the Increased Susceptibility to RA Teratogenesis Induced by Maternal Diabetes

Cyp26a1 is highly RA-inducible, as it contains multiple RA response elements (31). Thus,

as a proof of principle, we attempted to “pre-condition” embryos of MD mice using an exogenous subteratogenic RA dose to upregulate *Cyp26a1* expression in order to determine whether preconditioning could lead to a protective effect against RA teratogenesis. Previous findings showed that maternal oral administration of 2.5 mg/kg RA is sufficient to achieve near full rescue of midgestation mouse embryos lacking Raldh2, the principal RA synthetic enzyme (32). Therefore, we preconditioned pregnant mice with 0.625 or 1.25 mg/kg RA via oral feeding. These doses are far lower than the teratogenic range but yielded a dose-dependent increase in *Cyp26a1* mRNA levels in tailbuds of embryos by 2 h after administration (Fig. 6*A*). Notably, supplementation with 0.625 mg/kg RA did not induce changes in *Fgf8*, *Wnt3a*, and *Cdx2* expression (Supplementary Fig. 6), but upregulated the expression of *Cyp26a1* in tailbuds of the MD group to a level similar to that of the ND group fed the vehicle (Fig. 6*A*), with a concomitant normalization of RA-degrading efficiency (Fig. 6*B*). Then, when mothers were challenged with an intraperitoneal injection of a teratogenic dose of RA (25 mg/kg), we found the severity of caudal truncation to be significantly reduced, as shown by the significantly higher TL-to-CRL ratio in embryos of RA-preconditioned mice than in embryos from vehicle-fed mice in both the MD and ND conditions (Fig. 6*C*). Even the higher pre-conditioning dose of RA (1.25 mg/kg) was nonteratogenic and by itself did not affect the TL-to-CRL ratio of the embryo. While it could have had other effects on the embryo, in addition to upregulating *Cyp26a1*, the highly comparable pattern of dose-dependent upregulation of *Cyp26a1* and dose-dependent increase in the TL-to-CRL ratio, in the absence of changes in the key caudal regulatory genes suggests a specific effect of preconditioning. These findings support the idea that preconditioning the embryo by enhancing RA-degrading efficiency can offer a protective effect against RA

teratogenesis and abolish the increased propensity of embryos from pregnancy in diabetic mice toward RA-induced caudal truncation.

Amongst the most frequent congenital anomalies associated with maternal diabetes are neural tube defects (NTDs) (4). Expression levels of *Cyp26a1* in the cranial mesenchyme and the caudal neural plate are prominently reduced in E8 embryos of MD mice (Fig. 1*B*). Moreover, *Cyp26a1*$^{-/-}$ embryos exhibit exencephaly and spina bifida (13,14), suggesting the importance of the CYP26A1 enzyme in protecting these tissues from the deleterious effects of ectopic RA signaling. We found that injection of 25 mg/kg of RA at E8 induced around 6.7% exencephaly (Fig. 7*A*) and 4.4% spina bifida (Fig. 7*B*) in *Cyp26a1*$^{+/+}$ embryos of ND mice. However, the incidence of RA-induced exencephaly and spina bifida was markedly increased by six- and sevenfold, respectively, in *Cyp26a1*$^{+/+}$ embryos exposed to diabetes. A similar trend was found in embryos with an ICR X ICR background (Supplementary Fig. 7). The penetrance of NTDs was further exacerbated to 75.0% exencephaly and 71.3% spina bifida in *Cyp26a1*$^{+/-}$ embryos of MD mice with a preexisting genetic defect of RA catabolism. Similar to caudal truncation, the increase in susceptibility to RA-induced exencephaly and spina bifida caused by maternal diabetes was significantly reduced when embryos were preconditioned by maternal feeding of low-dose RA. Together, these findings support the idea that deregulated RA catabolism resulting from reduced levels of *Cyp26a1* expression acts to sensitize embryos of mothers with diabetes to fluctuations in RA levels.

DISCUSSION

In the present study, we found that the embryonic expression of the key RA-catabolizing enzyme *Cyp26a1* is significantly downregulated under the condition of maternal diabetes. This leads to a decrease in RA inactivation efficiency and enhances the deleterious effect of excessive RA signaling on key caudal regulatory genes, such as *Fgf8*, *Wnt3a*, and *Cdx2*, which are required for continued axial elongation (27). We previously demonstrated that enhanced RA-induced downregulation of *Wnt3a* exacerbated apoptosis in the tailbud of mouse embryos exposed to a diabetic or hyperglycemic condition, leading to premature termination of caudal development (18,33). This resulted in the absence of lower vertebrae, an imperforate anus, clubfeet, and renal and caudal spinal cord malformations, all of which are commonly associated with caudal regression (10,11,15-17).

The most frequent anomalies in pregnancies complicated by pregestational diabetes are NTDs and congenital heart defects (CHDs) (4,5). Results of this study support the idea that a decrease in *Cyp26a1* expression also significantly increases the propensity of embryos from pregnancies in mothers with diabetes toward exencephaly and spina bifida when RA homeostasis is perturbed. Although we have not examined heart development, *Cyp26a1* is expressed in cardiac neural crest cells and in the primitive heart tube and outflow tract, and *Cyp26a1*$^{-/-}$ embryos exhibit CHDs (13,14). Specific subgroups of CHD associated with improper RA signaling (8,9) are highly similar to those showing increased frequencies in the offspring of mothers with pregestational diabetes (4,34). As tight regulation of RA signaling is critical for many developmental processes, deregulated RA catabolism in early embryonic life can perturb the

development of multiple organ systems, which is in line with the finding that specific multiple congenital anomalies are common in affected offspring of mothers with pregestational diabetes (4,5).

In our colony of diabetic mice, around 5% of embryos developed NTDs. However, large variations in congenital malformation frequencies occur between different laboratories; the frequency of NTDs reaches over 50% in some reports (35). While genetic background affects the susceptibility to diabetic embryopathy (2,36), recent studies demonstrate that different types of rodent chow could significantly alter the frequency of NTDs in embryos of diabetic mice, which supports the idea that maternal diet is an important modifier of the penetrance of malformation (3). Individual risk of malformation therefore depends on the interaction between genetic and environmental influences, which affects the developmental threshold of gene expression for normal development.

Many genetic and environmental factors can affect embryonic RA homeostasis and signaling pathways to potentiate the effect of maternal diabetes in increasing malformation risk in the offspring. In humans, genetic polymorphisms of *CYP26A1* that exhibit significantly lower degrading efficiency of RA have been identified (37,38). Duplication and polymorphisms of the human *ALDH1A2* gene (encoding the principal RA synthetic enzyme during embryogenesis) are associated with an increase in serum RA levels (39) and various types of congenital anomalies, including CHDs and NTDs (40). Therefore common genetic variants involved in RA metabolism and signaling pathways could potentially be used as markers to identify pregnancies with increased malformation risk in mothers with diabetes.

Retinoids are recognized human teratogens (41). Various forms of retinoids are in

clinical use or under study for treating a variety of diseases, including skin disorders, obesity, diabetes, and related complications (42). A well-known example is isotretinoin (13-*cis* RA), which is prescribed for the treatment of severe acne. It has been shown that the teratogenic threshold for isotretinoin is much lower in humans (0.5 mg/kg) (43) than in mice (100 mg/kg) (44). Human embryos are highly sensitive to isotretinoin, with a pattern of malformations (8) similar to that seen in animals exposed to excess all-*trans* RA (9). In fact, the teratogenic effect of 13-*cis* RA has been demonstrated in animals and suggested to be mediated in humans via its conversion to all-*trans* RA, which then binds to nuclear RA receptors to regulate gene expression (45). Moreover, our previous studies (18) and the present report show that maternal diabetes can enhance RA teratogenicity. Thus the teratogenic threshold for isotretinoin in embryos of women with pregestational diabetes may be even lower than the 0.5 mg/kg threshold previously quoted (43).

Other than direct exposure to retinoids, medications such as valproic acid, an anticonvulsant, and fluconazole, used for treating fungal and yeast infections, have been shown to increase embryonic RA levels and induce malformations (46,47). Maternal smoking may also impose an increased risk; recent studies suggest that the teratogenic effect of nicotine on embryonic development is highly associated with suppression of *Cyp26a1* and perturbation of RA signaling (48). In fact, many chemicals can modulate RA homeostasis. As such, NTDs and axial defects mediated by the modulation of RA homeostasis are proposed to be adopted as an adverse Outcome Pathway (AOP) framework for assessing the developmental toxicity of chemicals (49).

There is a global trend that type 2 diabetes increasingly affecting children and adolescents (50). As the prevalence of diabetes among women of childbearing age continues to rise, the number of pregnancies complicated by pregestational diabetes is

likely to increase exponentially. The partial penetrance and variable expressivity of diabetic embryopathy underscore its multifactorial nature, implicating interactions between the genetic makeup of the embryo, maternal factors, and environmental influence. It is therefore of the utmost importance to identify risk factors in order to reduce malformations in pregnancy in women with diabetes. This study is, to our knowledge, the first to show that RA catabolism is deregulated in embryos exposed to diabetes and suggests that pregnancies in women with diabetes may be more vulnerable to perturbation in RA homeostasis and signaling. This may highlight the need to be cautious in assessing the upper safe levels of drugs, supplements, and potential teratogens-particularly those that have effects on RA homeostasis and signaling-for women with pregestational diabetes. Association studies should be conducted to determine whether specific genetic variants or periconceptional exposure to environmental agents that perturb RA homeostasis and signaling could be potentiation factors that increase individual malformation risk in the offspring of mothers with diabetes. Identifying these targets could contribute to genetic screening and preventive health care for women with diabetes with childbearing potential. Furthermore, as a proof of principle, we demonstrated the protective effect of correcting RA catabolism in embryos of diabetic mice. This finding may form the basis for developing stratified medicine to reduce the risk of congenital anomalies in pregnancies complicated by pregestational diabetes.

Acknowledgements. The authors thank Prof. Hiroshi Hamada of the RIKEN Center for Developmental Biology for the gift of *Cyp26a1* mutant mice and *Cyp26a1*, *Cyp26b1*, and *Cyp26c1* mouse cDNA plasmids; Johnson & Johnson Pharmaceutical Research & Development for the gift of R115866; and Dr. M. Wagner of the Howard Hughes Medical Institute for the gift of the RA reporter cell line. The authors thank the anonymous reviewers for their extensive and valuable input, which greatly improved the article.

Funding. This work was supported by funding from Hong Kong Research Grants Council General Research Fund (441606 and 474109 to Y.C.L., C.C.W., P.J.M., A.J.C., and A.S.W.S.).

Duality of Interest. No potential conflicts of interest relevant to this article were reported.

Author Contributions. L.M.Y.L. researched data and wrote the manuscript. M.B.W.L. and R.C.Y.K. researched data. Y.C.L. provided technical advice and contributed research materials. C.C.W contributed to discussion. P.J.M. provided technical advice, contributed research materials, and edited the manuscript. A.J.C. contributed to the discussion and edited the manuscript. A.S.W.S. designed the study and wrote the manuscript. A.S.W.S. is the guarantor of this work and, as such, had full access to all the data in this study and takes responsibility for the integrity of the data and the accuracy of the data analysis.

References

1. Correa A, Gilboa SM, Besser LM, et al. Diabetes mellitus and birth defects. Am J Obstet Gynecol 2008;199:237.e1-237.e9
2. Pani L, Horal M, Loeken MR. Polymorphic susceptibility to the molecular causes of neural tube defects during diabetic embryopathy. Diabetes 2002;51:2871-2874
3. Kappen C, Kruger C, MacGowab J, Salbaum JM. Maternal diet modulates the risk for neural tube defects in a mouse model of diabetic pregnancy. Reprod Toxicol 2011;31:41-49
4. Garne E, Loane M, Dolk H, et al. Spectrum of congenital anomalies in pregnancies with pregestational diabetes. Birth Defects Res A Clin Mol Teratol 2012;94:134-140
5. Martinez-Frias ML. Epidemiological analysis of outcomes of pregnancy in diabetic mothers: identification of the most characteristic and most frequent congenital anomalies. Am J Med Genet 1994;51:108-113
6. Kucera J. Rate and type of congenital anomalies among offspring of diabeticwomen. J Reprod Med 1971;7:73-82
7. Rothman KJ, Moore LL, Singer MR, Nguyen US, Mannino S, Milunsky A. Teratogenicity of high vitamin A intake. N Engl J Med 1995;333:1369-1373
8. Lammer EJ, Chen DT, Hoar RM, et al. Retinoic acid embryopathy. N Engl J Med 1985;313:837-841
9. Shenefelt RE. Morphogenesis of malformations in hamsters caused by retinoic acid: relation to dose and stage at treatment. Teratology 1972;5:103-118
10. Padmanabhan R. Retinoic acid-induced caudal regression syndrome in the mouse fetus. Reprod Toxicol 1998;12:139-151
11. Shum AS, Poon LL, Tang WW, et al. Retinoic acid induces down-regulation of Wnt-3a, apoptosis and diversion of tailbud cells to a neural fate in the mouse embryo. Mech Dev 1999;84:17-30
12. Fujii H, Sato T, Kaneko S, et al. Metabolic inactivation of retinoic acid by a novel P450 differentially expressed in developing mouse embryos. EMBO J 1997;16:4163-4173
13. Abu-Abed S, Dollé P, Metzger D, Beckett B, Chambon P, Petkovich M. The retinoic acid-metabolizing enzyme, CYP26A1, is essential for normal hindbrain patterning, vertebral identity, and development of posterior structures. Genes Dev 2001;15:226-240
14. Sakai Y, Meno C, Fujii H, et al. The retinoic acid-inactivating enzyme CYP26 is essential for establishing an uneven distribution of retinoic acid along the anterio-posterior axis within the mouse embryo. Genes Dev 2001;15:213-225
15. Tse HK, Leung MB, Woolf AS, et al. Implication of Wt1 in the pathogenesis of nephrogenic failure in a mouse model of retinoic acid-induced caudal regression syndrome. Am J Pathol 2005;166:1295-1307
16. Duhamel B. From the mermaid to anal imperforation: the syndrome of caudal regression. Arch Dis Child 1961;36:152-155
17. Pang D. Sacral agenesis and caudal spinal cord malformations. Neurosurgery 1993;32:755-778
18. Chan BW, Chan KS, Koide T, et al. Maternal diabetes increases the risk of caudal regression caused by retinoic acid. Diabetes 2002;51:2811-2816

19. Wilkinson DG. Whole mount in situ hybridization of vertebrate embryos. *In situ hybridization: A Practical Approach*. Wilkinson DG, Ed. Oxford, IRL Press, 1992, p. 75-83
20. Yamamoto M, Dräger UC, McCaffery P. A novel assay for retinoic acid catabolic enzymes shows high expression in the developing hindbrain. Brain Res Dev Brain Res 1998;107:103-111
21. Stoppie P. R115866 inhibits all-trans-retinoic acid metabolism and exerts retinoidal effects in rodents. J Pharmacol Exp Ther 2000;293:304-312
22. Wagner M, Han B, Jessell TM. Regional differences in retinoid release from embryonic neural tissue detected by an in vitro reporter assay. Development 1992;116:55-66
23. Schmidt CK, Brouwer A, Nau H. Chromatographic analysis of endogenous retinoids in tissues and serum. Anal Biochem 2003;315:36-48
24. Lee LM, Leung CY, Tang WW, et al. A paradoxical teratogenic mechanism for retinoic acid. Proc Natl Acad Sci U S A 2012;109:13668-13673
25. Tzimas G, Thiel R, Chahoud I, Nau H. The area under the concentration-time curve of all-trans-retinoic acid is the most suitable pharmacokinetic correlate to the embryotoxicity of this retinoid in the rat. Toxicol Appl Pharmacol 1997;143:436-444
26. Iulianella A, Beckett B, Petkovich M, Lohnes D. A molecular basis for retinoic acid-induced axial truncation. Dev Biol 1999;205:33-48
27. Neijts R, Simmini S, Giuliani F, van Rooijen C, Deschamps J. Region-specific regulation of posterior axial elongation during vertebrate embryogenesis. Dev Dyn 2014;243:88-98
28. Kumar S, Duester G. Retinoic acid controls body axis extension by directly repressing Fgf8 transcription. Development 2014;141:2972-2977
29. Lohnes D, Kastner P, Dierich A, Mark M, LeMeur M, Chambon P. Function of retinoic acid receptor gamma in the mouse. Cell 1993;73:643-658
30. Kastner P, Mark M, Ghyselinck N, et al. Genetic evidence that the retinoid signal is transduced by heterodimeric RXR/RAR functional units during mouse development. Development 1997;124:313-326
31. Zhang Y, Zolfaghari R, Ross AC. Multiple retinoic acid response elements cooperate to enhance the inducibility of CYP26A1 gene expression in liver. Gene 2010;464:32-43
32. Niederreither K, Subbarayan V, Dollé P, Chambon P. Embryonic retinoic acid synthesis is essential for early mouse post-implantation development. Nat Genet 1999;21:444-448
33. Leung MB, Choy KW, Copp AJ, Pang CP, Shum AS. Hyperglycaemia potentiates the teratogenicity of retinoic acid in diabetic pregnancy in mice. Diabetologia 2004;47:515-522
34. Lisowski LA, Verheijen PM, Copel JA, et al. Congenital heart disease in pregnancies complicated by maternal diabetes mellitus. An international clinical collaboration, literature review, and meta-analysis. Herz 2010;35:19-26
35. Fine EL, Horal M, Chang T, Fortin G, Loeken MR. Evidence that elevated glucose causes altered gene expression, apoptosis, and neural tube defects in a mouse model of diabetic pregnancy. Diabetes 1999;48:2454-2562
36. Ejdesjö A, Wentzel P, Eriksson UJ. Genetic and environmental influence on

diabetic rat embryopathy. Am J Physiol Endocrinol Metab 2011;300:E454-467
37. Lee SJ, Perera L, Coulter SJ, Mohrenweiser HW, Jetten A, Goldstein JA. The discovery of new coding alleles of human CYP26A1 that are potentially defective in the metabolism of all-trans retinoic acid and their assessment in a recombinant cDNA expression system. Pharmacogenet Genomics 2007; 17:169-180
38. Rat E, Billaut-Laden I, Allorge D, et al. Evidence for a functional genetic polymorphism of the human retinoic acid-metabolizing enzyme CYP26A1, an enzyme that may be involved in spina bifida. Birth Defects Res A Clin Mol Teratol 2006;76:491-498
39. El Kares R, Manolescu DC, Lakhal-Chaieb L, et al. A human ALDH1A2 gene variant is associated with increased newborn kidney size and serum retinoic acid. Kidney Int 2010;78:96-102
40. Deak KL, Dickerson ME, Linney E, et al. Analysis of ALDH1A2, CYP26A1, CYP26B1, CRABP1, and CRABP2 in human neural tube defects suggests a possible association with alleles in ALDH1A2. Birth Defects Res A Clin Mol Teratol 2005;73:868-875
41. Soprano DR, Soprano KJ. Retinoids as teratogens. Annu Rev Nutr 1995;15:111-132
42. Villarroya F, Iglesias R, Giralt M. Retinoids and retinoid receptors in the control of energy balance: novel pharmacological strategies in obesity and diabetes. Curr Med Chem 2004;11:795-805
43. Rosa FW, Wilk AL, Kelsey FO. Teratogen update: vitamin A congeners. Teratology 1986;33:355-364
44. Kraft JC, Kochhar DM, Scott WJ, Nau H. Low teratogenicity of 13-cis-retinoic acid (isotretinoin) in the mouse corresponds to low embryo concentrations during organogenesis: comparison to the all-trans isomer. Toxicol Appl Pharmacol 1987;87:474-482
45. Nau H. Teratogenicity of isotretinoin revisited: species variation and the role of all-trans-retinoic acid. J Am Acad Dermatol 2001;45:S183-187
46. Chuang CM, Chang CH, Wang HE, et al. Valproic acid downregulates RBP4 and elicits hypervitaminosis A-teratogenesis - a kinetic analysis on retinol/retinoic acid homeostatic system. PLoS One 2012;7:e43692
47. Di Renzo F, Broccia ML, Giavini E, Menegola E. Citral, an inhibitor of retinoic acid synthesis, attenuates the frequency and severity of branchial arch abnormalities induced by triazole-derivative fluconazole in rat embryos cultured in vitro. Reprod Toxicol 2007;24:326-332
48. Feltes BC, de Faria Poloni J, Notari DL, Bonatto D. Toxicological effects of the different substances in tobacco smoke on human embryonic development by a systems chemo-biology approach. PLoS One 2013;8:e61743
49. Tonk EC, Pennings JL, Piersma AH. An adverse outcome pathway framework for neural tube and axial defects mediated by modulation of retinoic acid homeostasis. Reprod Toxicol 2015;55:104-113
50. Reinehr T. Type 2 diabetes mellitus in children and adolescents. World J Diabetes 2013;4:270-281

Table 1 - Frequency of various phenotypes (categorized according to the severity of malformations) induced by in vivo challenge with 40 mg/kg RA at E9 in *Cyp26a1* heterozygous null (+/-) and wild-type (+/+) fetuses from ND and MD mice at E18

	Fetuses from ND mothers (n = 11 litters)		Fetuses from MD mothers (n = 11 litters)	
Genotype	+/+	+/-	+/+	+/-
Live fetuses (n)	68	61	48	49
Fetuses with two normal kidneys (%)	91.2	80.3	62.5	36.7
Nonagenesis renal malformation (%)				
Unilateral (with a normal contralateral kidney)	2.9	9.8	16.7	26.5
Bilateral	2.9	8.2	12.5	10.2
Renal agenesis (%)				
Unilateral				
The solitary kidney is normal	1.5	1.6	0	8.2
The solitary kidney has nonagenesis malformations	1.5	0	4.2	6.1
Bilateral	0	0	4.2	12.2

FIGURE LEGENDS

Figure 1 - Embryos of diabetic mice exhibit specific downregulation of *Cyp26a1*. *A-D, F*, and *H*: Whole-mount in situ hybridization patterns of *Cyp26* genes in embryos of MD mice compared with those of ND mice. *Cyp26a1* mRNA transcripts are seen in extraembryonic endoderm (red arrowhead) and headfold mesenchyme (yellow arrowhead) of E7 conceptuses (*A*); cranial mesenchyme (green arrowhead) and caudal neural plate (orange arrowhead) of E8 embryos (*B*); craniofacial, cervical, and branchial arch mesenchyme (circled) (*C*); and tailbud (blue arrowhead) of E9 embryos (*D*). *Cyp26b1* (*F*) and *Cyp26c1* (*H*) are expressed in the cranial but not in the tailbud region of E9 embryos. At least 20 embryos from five or six litters were examined for each group. Scale bar = 0.05 mm (*A*), 0.1 mm (*B*), 0.7 mm (*C*), 0.2 mm (*D*), 0.7 mm for the whole embryo and 0.35 mm for the caudal region (*F* and *H*). *E*,*G*, and *I*: Quantification of mRNA levels of *Cyp26a1* (*E*), *Cyp26b1* (*G*), and *Cyp26c1* (*I*), normalized to *β-actin* and expressed relative to ND, which was set as 1 ($n = 5$ from five litters). *$P < 0.05$, Student *t* test. Error bars represent the mean ± SEM.

Figure 2 - Embryos of diabetic mice show reduced efficiency of RA catabolism. *A*: In vitro RA-degrading efficiency, presented as the percentage of RA in the medium being degraded by the tailbud lysate, in the presence or absence of the cofactor (NADPH) and the reducing agent (DTT) for optimal activity of CYP26 enzymes, and varying concentrations of R115866 (CYP26 inhibitor) ($n = 18$ in ND and MD groups with NADPH-DTT; $n = 3$-9 in other groups from 20 ND and 18 MD litters). *$P < 0.001$,

Student *t* test; $^{\dagger}R^2$ = 0.742 and *P* = 0.001, linear regression. *B*: In vivo RA clearance measured as the amount of RA released from individual tailbuds, using a RA reporter cell line, at hourly intervals after injection of 50 mg/kg RA at E9 (*n* = 16-42 from three to eight litters). **P* < 0.001 vs ND, Student *t* test and nonlinear regression. Error bars represent the mean ± SEM.

Figure 3 – Increased levels of endogenous RA are detected in tailbuds of E9 embryos of diabetic mice using a RA reporter cell line. *A*: Image illustrates the caudal-most portion of the tailbud (boundary marked by the dotted line) as excised for detection of bioactive RA. *B*: Percentage of tailbuds excised from embryos of ND and MD mice that have different numbers of positively stained cells induced in the RA reporter cell line (*n* = 19 for ND and 22 for MD from three and four litters, respectively). *C*: Representative images of excised tailbuds that were placed directly on the RA reporter cells and have different numbers of stained cells induced in the RA reporter cell line. The amount of stained cells is categorized as (-), (+), (++) and (+++) as defined in *B*.

Figure 4 - Tailbuds of E9 embryos of diabetic mice exhibit a greater magnitude of suppression of key genes for caudal development induced by RA. *A*: Quantification of mRNA levels of various caudal regulatory genes and RA nuclear receptors, normalized to *β-actin* and expressed relative to ND, which was set as 1, in tailbuds of embryos of ND and MD mice at E9 (*n* = 5 from five litters). ***P* < 0.01, Student *t* test. *B* and *C*: Quantification of mRNA levels of *Cyp26a1* (*B*), and various caudal regulatory genes and RA nuclear receptors (*C*), normalized to *β-actin* and expressed relative to ND (CON),

which was set as 1, in tailbuds of embryos of ND and MD mice 4 h after injection of 50 mg/kg RA (50RA) or vehicle as control (CON) into the mothers at E9 (n = 5 from five litters). *P < 0.05; **P < 0.01; ***P < 0.001, one-way ANOVA followed by the Bonferroni test. Error bars represent the mean ± SEM.

Figure 5 - *Cyp26a1* loss-of-function genotype interacts with diabetic maternal environment to influence RA-degrading efficiency and susceptibility to RA teratogenesis. *A*: Whole-mount in situ hybridization patterns of *Cyp26a1* expression in *Cyp26a1* heterozygous null (+/-) embryos and their wild-type (+/+) littermates from ND and MD mice at E9. At least 30 embryos from six to eight litters were examined for each group. Scale bar = 0.25 mm. *B*: Quantification of *Cyp26a1* mRNA, normalized to *β-actin* and expressed relative to ND (+/+), which was set as 1, in tailbuds of embryos from different genotype-maternal environment combinations at E9 (n = 5 from five litters). *C*: In vitro RA-degrading efficiency, presented as the percentage of RA in the medium being degraded by the tailbud lysate in the absence or presence of 100 nmol/L R115866 (a CYP26 inhibitor) (n = 8-13 from 10 to 14 litters). *D*: Quantification of RA released from individual tailbuds, using a RA reporter cell line, 3 h after in vivo challenge with 25 mg/kg RA (25RA) at E9 (n = 22-28 from six to seven litters). *E*: Maternal injection of 25RA or vehicle as the control (CON) at E9. Caudal truncation, measured in terms of the ratio of TL to CRL (TL/CRL), was examined in E13 embryos (n = 41-62 from 10 litters). *F*: Maternal injection of 40 mg/kg RA (40RA) or CON at E9. Near-term E18 fetuses were examined for renal malformations (n = 11 litters). *P < 0.05; **P < 0.01; ***P < 0.001, one-way ANOVA followed by the Bonferroni test. Error bars represent the mean ± SEM.

Figure 6 - Preconditioning with low-dose RA up-regulates *Cyp26a1*, increases RA-degrading efficiency, and protects against RA-induced caudal truncation. *A*: Quantification of *Cyp26a1* mRNA, normalized to *β-actin* and expressed relative to ND (control [CON]), which was set as 1, in tailbuds of E9 embryos from ND and MD mice 2 h after maternal oral feeding with low-dose RA (0.625 mg/kg [0.625RA] or 1.25 mg/kg [1.25RA]), or with vehicle as the control (n = 5 from five litters). *B*: In vitro RA-degrading efficiency, presented as the percentage of RA in the medium being degraded by the tailbud lysate from embryos with or without preconditioned with 0.625RA (n = 5 from three to five litters). *C*: Embryos, preconditioned with low-dose RA or not, were maternally challenged with a teratogenic dose of 25 mg/kg RA (25RA) via administration to the mother at E9, and were examined for caudal truncation, measured in terms of the ratio of TL to CRL (TL/CRL) at E13 (n = 34-60 from three to five litters). *P < 0.01; **P < 0.001, Student t test. $^{\dagger}R^2$ = 0.900 and P < 0.001; $^{\dagger\dagger}R^2$ = 0.869 and P < 0.001; $^{\dagger\dagger\dagger}R^2$ = 0.610 and P < 0.001; $^{\dagger\dagger\dagger\dagger}R^2$ = 0.729 and P < 0.001, linear regression. The dotted lines represent no significant difference between the two groups. Error bars represent the mean ± SEM.

Figure 7 - Increased susceptibility of embryos of diabetic mice to RA-induced NTDs is abolished by preconditioning with low-dose RA. *A* and *B*: Incidence rates of exencephaly (*A*) and spina bifida (*B*) in E13 *Cyp26a1* heterozygous null (+/-) and wild-type (+/+) embryos from ND and MD mice (n = 8-9 litters). Effect of preconditioning by oral feeding of low-dose RA (0.625 mg/kg [0.625RA]) is compared with the vehicle-fed

control (CON) or no treatment (NT) groups, 2 h before in vivo challenge with a teratogenic dose of 25 mg/kg RA (25RA) at E8. *$P < 0.05$; **$P < 0.01$; ***$P < 0.001$, one-way ANOVA followed by the Bonferroni test. The dotted lines represent no significant difference between the two groups. Error bars represent the mean ± SEM.

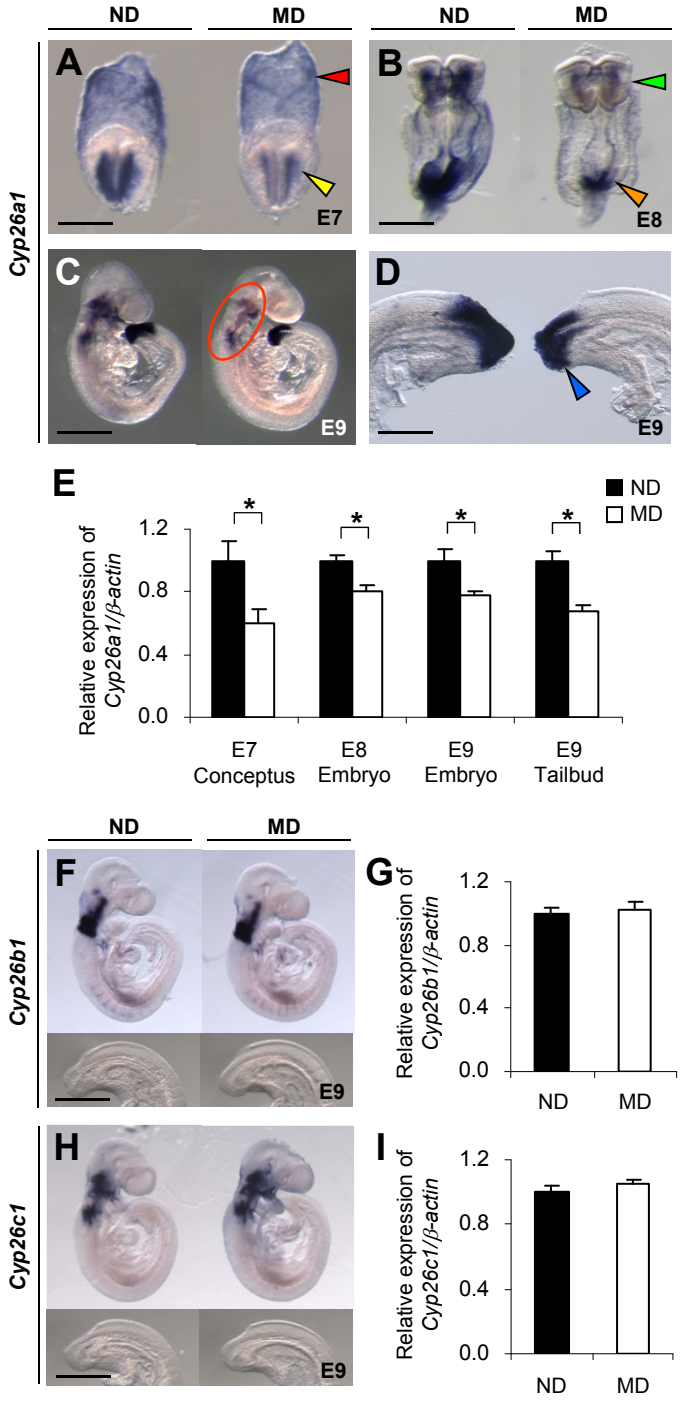
ND
MD
ND
MD
Cyp26a1
A
B
E7
E8
C
D
E9
E9
E
ND
MD
Relative expression of Cyp26a1/β-actin
1.2
0.8
0.4
0.0
*
*
*
*
E7 Conceptus
E8 Embryo
E9 Embryo
E9 Tailbud
ND
MD
Cyp26b1
F
E9
G
Relative expression of Cyp26b1/β-actin
1.2
0.8
0.4
0.0
ND
MD
Cyp26c1
H
E9
I
Relative expression of Cyp26c1/β-actin
1.2
0.8
0.4
0.0
ND
MD

Figure 1

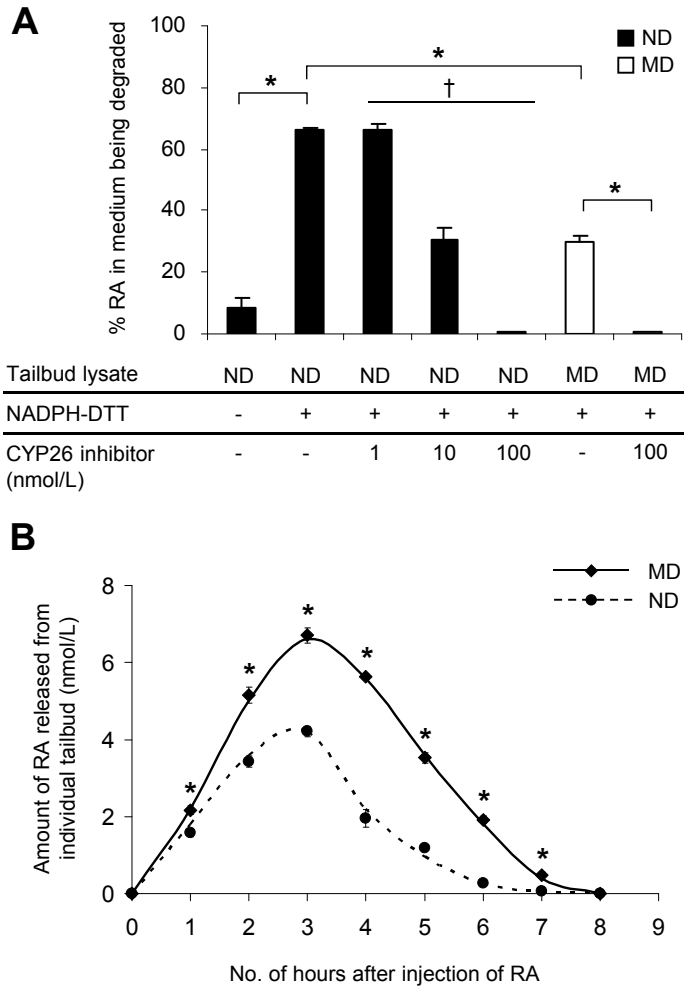
A
% RA in medium being degraded
100
80
60
40
20
0
ND
MD
*
*
†
*
Tailbud lysate ND ND ND ND ND MD MD
NADPH-DTT - + + + + + +
CYP26 inhibitor (nmol/L) - - 1 10 100 - 100
B
Amount of RA released from individual tailbud (nmol/L)
8
6
4
2
0
MD
ND
0 1 2 3 4 5 6 7 8 9
No. of hours after injection of RA

Figure 2

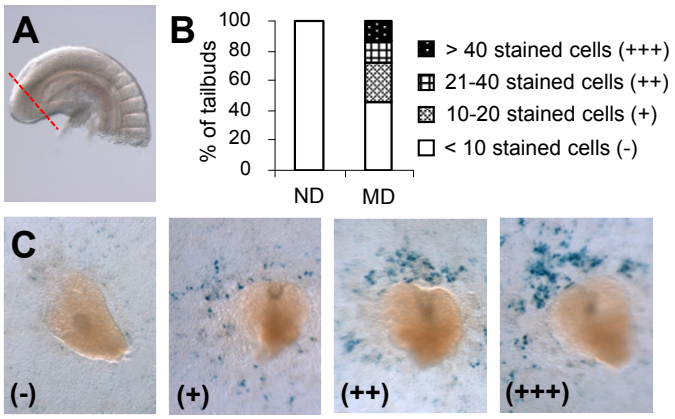
A
B
100
80
60
40
20
0
% of tailbuds
ND
MD
> 40 stained cells (+++)
21-40 stained cells (++)
10-20 stained cells (+)
< 10 stained cells (-)
C
(-)
(+)
(++)
(+++)

Figure 3

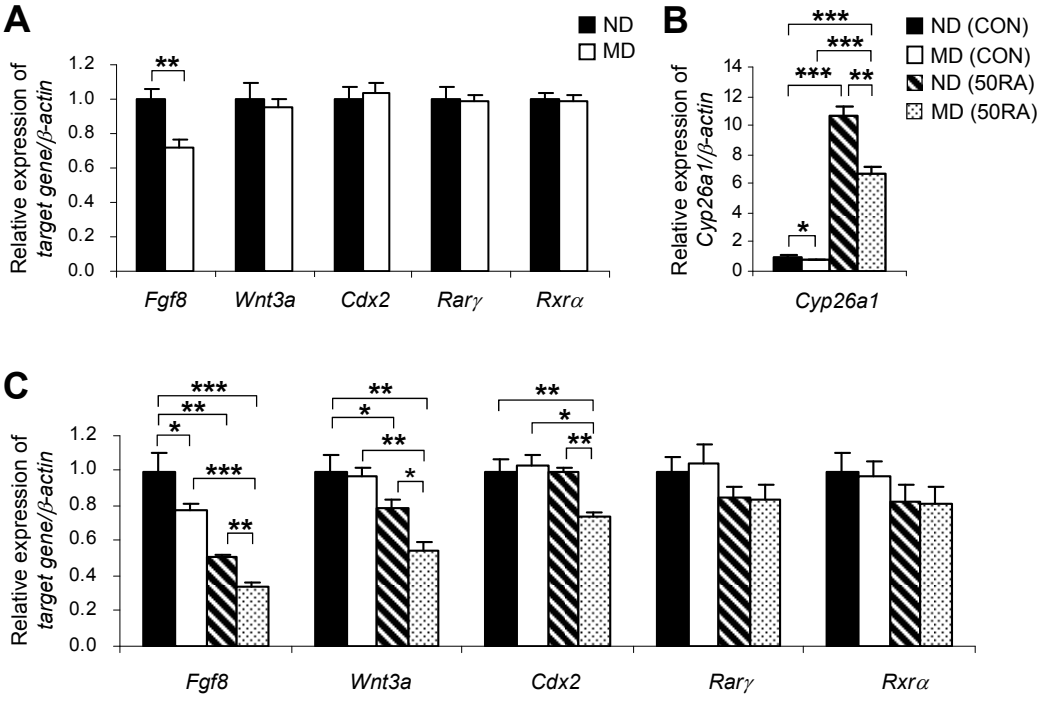
A
ND
MD
Relative expression of target gene/β-actin
1.2
1.0
0.8
0.6
0.4
0.2
0.0
**
Fgf8
Wnt3a
Cdx2
Rarγ
Rxrα
B
ND (CON)
MD (CON)
ND (50RA)
MD (50RA)
Relative expression of Cyp26a1/β-actin
14
12
10
8
6
4
2
0
***
***
***
**
*
Cyp26a1
C
Relative expression of target gene/β-actin
1.2
1.0
0.8
0.6
0.4
0.2
0.0
***
**
*
***
**
**
*
**
*
**
**
*
**
Fgf8
Wnt3a
Cdx2
Rarγ
Rxrα

Figure 4

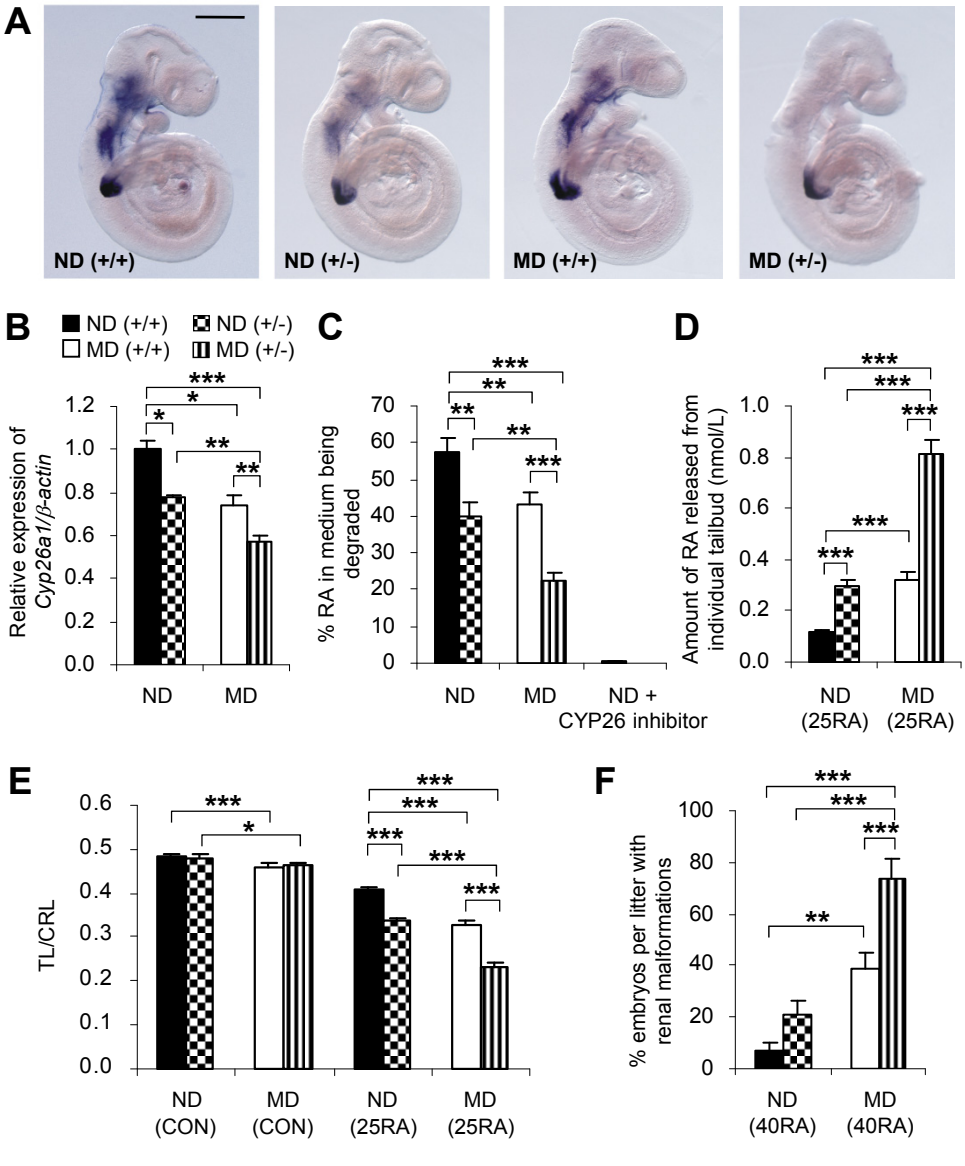
A
ND (+/+)
ND (+/-)
MD (+/+)
MD (+/-)
B
ND (+/+)
ND (+/-)
MD (+/+)
MD (+/-)
Relative expression of Cyp26a1/β-actin
ND
MD
C
% RA in medium being degraded
ND
MD
ND + CYP26 inhibitor
D
Amount of RA released from individual tailbud (nmol/L)
ND (25RA)
MD (25RA)
E
TL/CRL
ND (CON)
MD (CON)
ND (25RA)
MD (25RA)
F
% embryos per litter with renal malformations
ND (40RA)
MD (40RA)

Figure 5

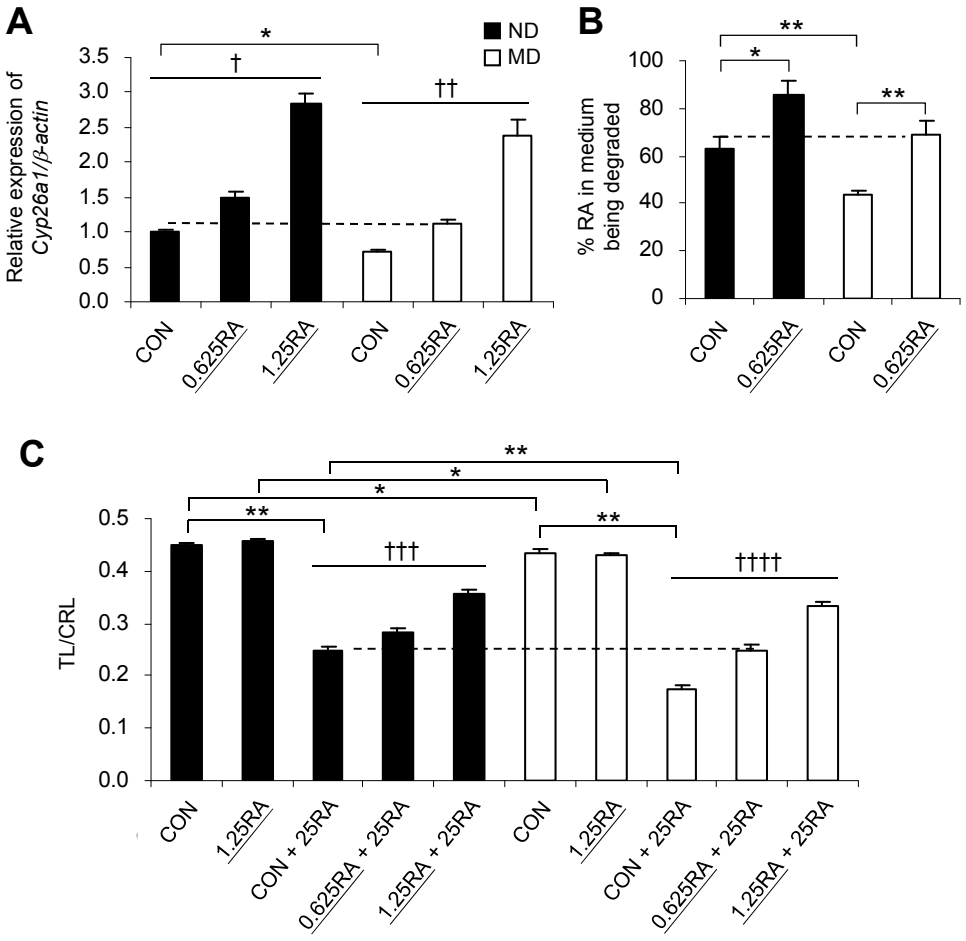
A
ND
MD
Relative expression of Cyp26a1/β-actin
3.5
3.0
2.5
2.0
1.5
1.0
0.5
0.0
*
†
††
CON
0.625RA
1.25RA
CON
0.625RA
1.25RA
B
% RA in medium being degraded
100
80
60
40
20
0
**
*
**
CON
0.625RA
CON
0.625RA
C
TL/CRL
0.5
0.4
0.3
0.2
0.1
0.0
**
*
*
**
**
†††
††††
CON
1.25RA
CON + 25RA
0.625RA + 25RA
1.25RA + 25RA
CON
1.25RA
CON + 25RA
0.625RA + 25RA
1.25RA + 25RA

Figure 6

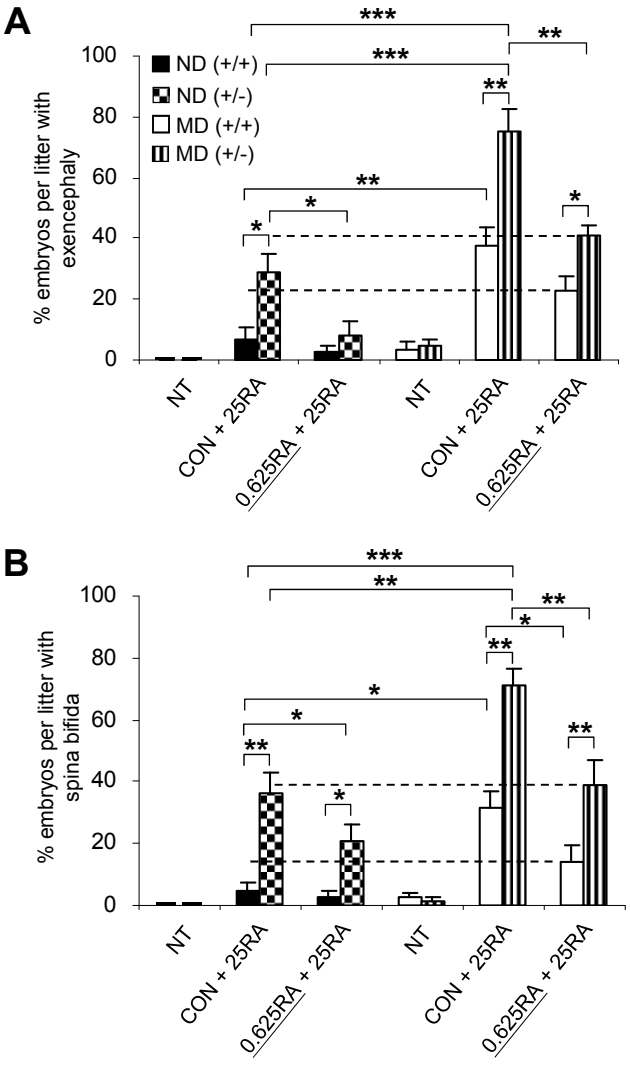
A
B
ND (+/+)
ND (+/-)
MD (+/+)
MD (+/-)
% embryos per litter with exencephaly
% embryos per litter with spina bifida
100
80
60
40
20
0
NT
CON + 25RA
0,625RA + 25RA
NT
CON + 25RA
0,625RA + 25RA
***
**
*

Figure 7

Supplementary Figure 1. A representative standard curve showing the response of the RA reporter cell line to serially diluted RA solutions from 10^{-6} to 10^{-11} mol/L. There is a linear dose-response from 10^{-7} to 10^{-10} mol/L RA. The RA concentration of the sample is within the linear section of the standard curve. R^2 represents the coefficient of determination for linear regression analysis.

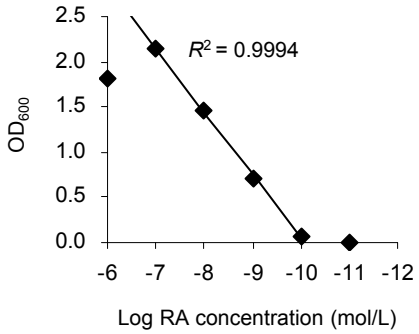

Supplementary Figure 2. RA was stable at 37°C for 24 h. RA was added to the culture medium at a concentration of 10 nmol/L. The medium was either immediately frozen and stored at -80°C (n = 4) or incubated at 37°C for 24 h in a 5% CO_2 incubator (n = 4). The RA concentrations of the two groups of samples were then determined by the RA reporter cell line. There was no significant degradation of RA in the sample that had been incubated at 37°C for 24 h in comparison to the immediately frozen sample.

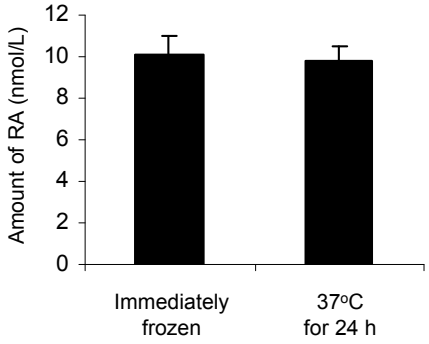

Supplementary Figure 3. No significant difference in the protein content of the tailbuds excised from embryos of ND and MD mice. Total protein in individual tailbuds measured using Bradford assay (n = 18-20 from three litters). Error bars represent the mean ± SEM.

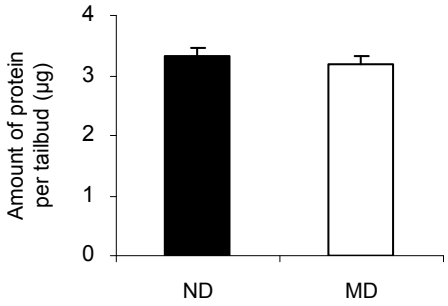

Supplementary Figure 4. The midbrain, which does not express any of the three *Cyp26* genes, exhibits no difference in RA levels between embryos of MD and ND mice after RA treatment. *A*: Whole-mount in situ hybridization patterns showed that all three *Cyp26* genes (*Cyp26a1*, *Cyp26b1*, and *Cyp26c1*) did not express in the midbrain (MB) of E9 embryos of mice with or without (No RA) treatment of 50 mg/kg RA (50RA). Scale bar = 0.4 mm. *B*: Amount of RA in the tailbud and midbrain of E9 embryos 3 h after injection of 50RA, measured using high-performance liquid chromatography (n = 7 for ND and 9 for MD from seven and nine litters, respectively). The tailbud of embryos of MD mice with reduced *Cyp26a1* expression had a significantly greater amount of RA than that in embryos of ND mice. In contrast, the midbrain, without *Cyp26* expression, showed no difference in the amount of RA between embryos of MD and ND mice. *P < 0.001, Student t test. Error bars represent the mean ± SEM.

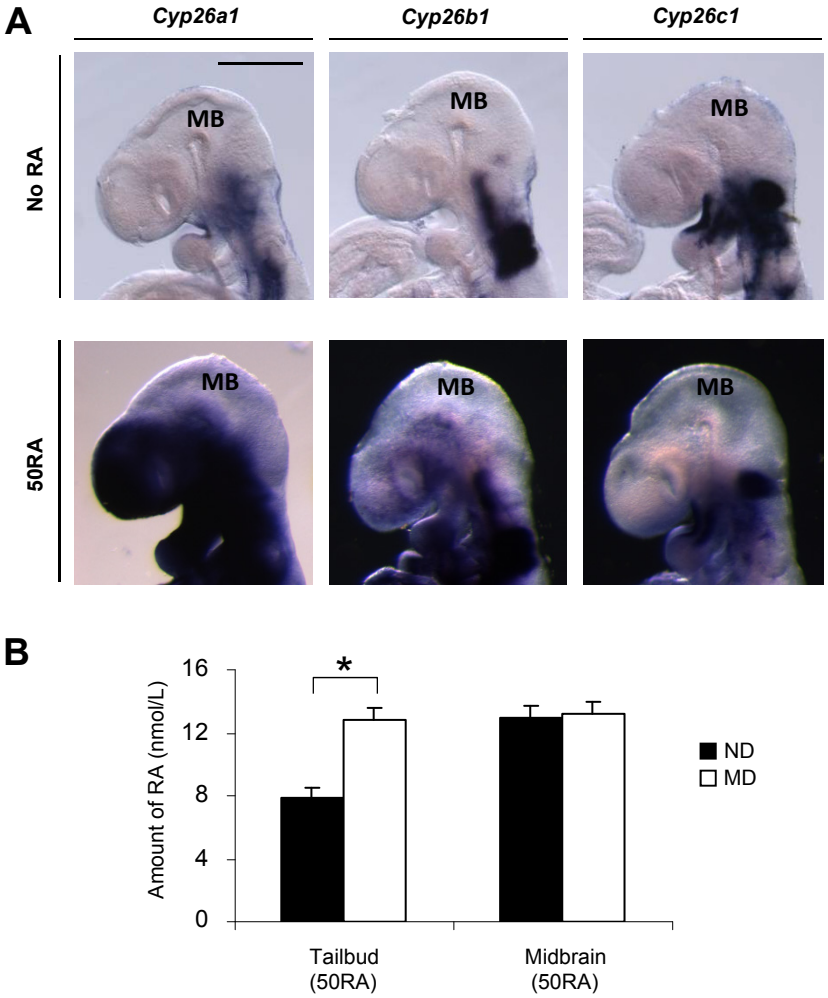

Supplementary Figure 5. Heterozygosity for *Cyp26a1* loss-of-function exacerbates increased susceptibility to RA-induced caudal truncation in embryos exposed to diabetes. Morphology of the caudal region of E13 *Cyp26a1* heterozygous null (+/-) embryos and their wild-type (+/+) littermates from ND and MD mice challenged with 25 mg/kg RA (25RA) or vehicle as control (CON) at E9. Embryos of different genotype-maternal environment combinations showed prominent differences in susceptibility to RA-induced caudal truncation. Scale bar = 0.1 cm.

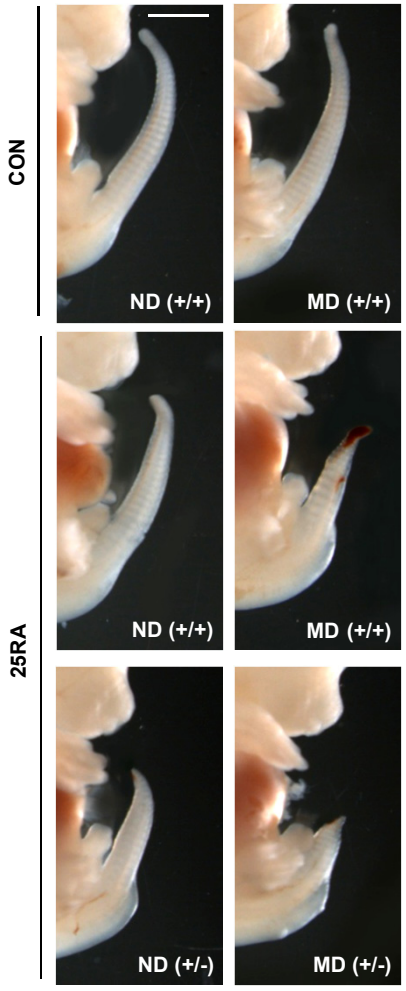

Supplementary Figure 6. Oral feeding of low-dose RA does not cause any change in expression of key genes for caudal development. Quantification of mRNA levels of various caudal regulatory genes, normalized to *β-actin,* and expressed relative to ND (CON), which was set as 1, in the tailbuds of E9 embryos from ND and MD mice 2 h after oral feeding with low-dose RA (0.625 mg/kg RA [0.625RA]) or with vehicle as the control (CON) (n = 5 from 5 litters). No significant changes in mRNA levels were associated with low-dose RA treatment. *P < 0.05, one-way ANOVA followed by the Bonferroni test. Error bars represent the mean ± SEM.

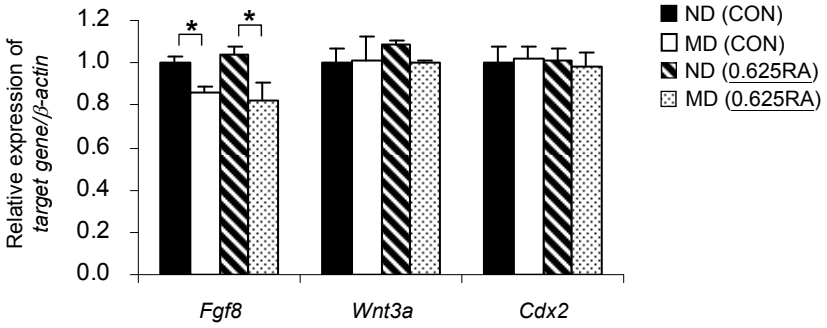

Supplementary Figure 7. Incidence of exencephaly in E13 embryos (ICR X ICR genetic background) from ND and MD mice with or without (No RA) in vivo challenge with 25 mg/kg RA (25RA) at E8 (n = 9-12 litters). In untreated conditions, only 3% of embryos of MD mice developed exencephaly. However, when challenged with 25RA, a dose that only induced exencephaly in 3% of embryos of ND mice, embryos of MD mice were significantly more susceptible to RA teratogenesis and exhibited a ninefold increase in the incidence rate of exencephaly. *P < 0.001, one-way ANOVA followed by the Bonferroni test. Error bars represent the mean ± SEM.

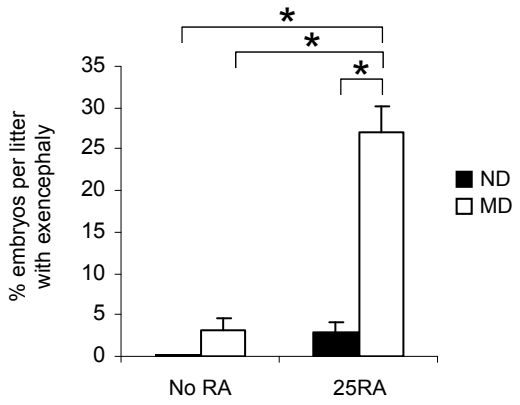

Supplementary Table 1. Blood glucose levels of ND and MD mice before pregnancy and on the day of embryo collection

	ND Before pregnancy	**ND** Day of embryo collection (E9)	**MD** Before pregnancy	**MD** Day of embryo Collection (E9)
Blood glucose levels (mmol/L) mean ± SEM	Not determined	6.08 ± 0.12 (*n* = 12)	21.56 ± 0.32 (*n* = 101)	27.53 ± 0.51* (*n* = 67)

Remarks:
The blood glucose levels of MD mice on the day of embryo collection at E9 were significantly higher than that of MD mice before pregnancy (*$P < 0.001$, Student *t* test), with none of them having blood glucose levels lower than 16.7 mmol/L. Similarly, there were hardly any MD mice exhibiting blood glucose levels lower than 16.7 mmol/L on the day of embryo collection at other stages (E8, E13 and E18). These findings supported that embryos of MD mice were exposed to a hyperglycemic milieu throughout development.

Supplementary Table 2. PCR conditions and primer sequences

The PCR conditions included initiation at 95^{o}C for 10 min, followed by 40 cycles comprising of denaturation at 95°C for 15 sec, annealing at 55°C for 30 sec and extension at 72°C for another 30 sec. Primers sequences, designed by Primer Express Software (Applied Biosystems), for detecting various mouse genes were:

Gene	**Primer Sequences**
β-actin	forward: 5'-TGT TAC CAA CTG GGA CGA CA-3' reverse: 5'-GGG GTG TTG AAG GTC TCA AA-3'
Cdx2	forward: 5'-AAA CTC CAC TGT CAC CCA GT-3' reverse: 5'-CCT GAG GTC CAT AAT TCC AC-3'
Cyp26a1	forward: 5'-CAG TGC TAC CTG CTC GTG AT-3' reverse: 5'-AGA GAA GAG ATT GCG GGT CA-3'
Cyp26b1	forward: 5'-TTC AGT GAG GCA AGA AGA CA-3' reverse: 5'-CTG GGA GGA GGT GCT AAG TA-3'
Cyp26c1	forward: 5'-GGG ACC AGT TGT ATG AGC AC-3' reverse: 5'-AGC CAA CTC CTT CAG CTC TT-3'
Fgf8	forward: 5'-AGA GAT CGT GCT GGA GAA CA-3' reverse: 5'-AAG GGC GGG TAG TTG AGG AA-3'
Rarγ	forward: 5'-AGG CAG CAG ACT GAC CAT TT-3' reverse: 5'-TTC TGG TAG GTG TGC AGC AG-3'
Rxrα	forward: 5'-TCA CCA TCC TCG CCA TCT TT-3' reverse: 5'-CTC CAA ACA GAG GTG CCA TG-3'
Wnt3a	forward: 5'-CTG GCA GCT GTG AAG TGA AG-3' reverse: 5'-GCC TCG TAG TAG ACC AGG TC-3'

Supplementary Table 3. The amount of RA in individual tailbuds of embryos of ND and MD mice 3 h after injection of 50 mg/kg RA at E9, measured using the RA reporter cell line or high-performance liquid chromatography (HPLC)

	Amount of RA per tailbud (nmol/L)		
	ND	**MD**	**Difference between ND and MD**
RA reporter cell line	4.21 ± 0.13 (n = 36)*	6.71 ± 0.20 (n = 42)*	59.38%
HPLC	7.88 ± 0.62 (n = 7)**	12.80 ± 0.79 (n = 9)**	62.44%

* One tailbud in each sample

** Tailbuds from one litter of embryos were pooled as one sample

Remarks:
The data for the RA reporter cell line was extracted from Fig. 2*B*.
The HPLC experiment was conducted in a separate study to validate the result in Fig. 2*B*.
In analyzing the result, it is more relevant to compare the difference between ND and MD groups using the two RA detection methods, rather than the absolute amount of RA in the tailbud.